



ELSEVIER

Contents lists available at ScienceDirect

Biosensors and Bioelectronics

journal homepage: www.elsevier.com/locate/bios

Visual and sensitive detection of viable pathogenic bacteria by sensing of RNA markers in gold nanoparticles based paper platform



Hongxing Liu, Fangfang Zhan, Fang Liu, Minjun Zhu, Xiaoming Zhou*, Da Xing*

MOE Key Laboratory of Laser Life Science & Institute of Laser Life Science, College of Biophotonics, South China Normal University, Guangzhou 510631, China

ARTICLE INFO

Article history:

Received 21 March 2014

Received in revised form

5 June 2014

Accepted 10 June 2014

Available online 14 June 2014

Keywords:

Pathogenic bacteria

RNA amplification

Listeria monocytogenes

Bioactive paper-based platform

ABSTRACT

Food-borne pathogens have been recognized as a major cause of human infections worldwide. Their identification needs to be simpler, cheaper and more reliable than the traditional methods. Here, we constructed a low-cost paper platform for viable pathogenic bacteria detection with the naked eye. In this study, an effective isothermal amplification method was used to amplify the *hlyA* mRNA gene, a specific RNA marker in *Listeria monocytogenes*. The amplification products were applied to the paper-based platform to perform a visual test using sandwich hybridization assays. When the RNA products migrated along the platform by capillary action, the gold nanoparticles accumulated at the designated area. Under optimized experimental conditions, as little as 0.5 pg/ μ L genomic RNA from *L. monocytogenes* could be detected. It could also be used to specifically detect 20 CFU/mL *L. monocytogenes* from actual samples. The whole assay process, including RNA extraction, amplification, and visualization, can be completed within several hours. This method is suitable for point-of-care applications to detect food-borne pathogens, as it can overcome the false-positive results caused by amplifying nonviable *L. monocytogenes*. Furthermore, the results can be imaged and transformed into a two-dimensional bar code through an Android-based smart phone for further analysis or in-field food safety tracking.

© 2014 Elsevier B.V. All rights reserved.

1. Introduction

Developing a rapid and affordable biosensor that can be used to detect food-borne pathogens such as *Listeria monocytogenes*, which has been an emerging pathogen since the late 1970s, remains a significant challenge (Hamon et al., 2006). This facultative intracellular food-borne pathogen has been responsible for outbreaks of listeriosis, a severe infection that primarily affects immune-compromised individuals, including pregnant women, newborns, and elderly people. Manifestations of listeriosis range from influenza-like illness to severe complications, including meningitis, septicemia, spontaneous abortion and a high fatality rate (30%) (Cossart and Toledo-Arana, 2008; Birmingham et al., 2008; Ribet et al., 2010). In recent years, several large listeriosis outbreaks have been associated with contaminated food such as vegetables, dairy products, soft cheeses, pasteurized milk and meat products. The incidence of food poisoning caused by the intake of food contaminated with *L. monocytogenes* is still increasing, and it has caused widespread concern in many countries (Rood, 2010). Therefore, it is critical to develop a low-cost, specific and highly sensitive method for detecting *L. monocytogenes*,

particularly in areas with poor resources such as villages in developing countries.

To identify *L. monocytogenes* in a food sample, conventional methods use one or more culture-based enrichment steps followed by plating onto a selective agar. These methods are sensitive and inexpensive, and they are the recommended standard for *L. monocytogenes* isolation; however, they are labor-intensive, time consuming and not always reliable (Zunabovic et al., 2011; Rivoal et al., 2013; Shafiee et al., 2013; Hsu et al., 2014). Therefore, a large number of tests based on the specific binding of an antibody to an antigen, such as enzyme-linked immunosorbent assays (ELISAs) (Zunabovic et al., 2011; Hsu et al., 2014) and immunochromatographic lateral flow test strips (Nash et al., 2012; Yan et al., 2012; Ge et al., 2012; Cho and Irudayaraj, 2013), have been developed. However, rapid immune tests, which are widely used in low-resource settings, are not appropriate for early food-borne pathogen detection because of their low sensitivity. Moreover, nonspecific immune responses can easily occur once the surroundings change dramatically, which can lead to a false-positive result.

To overcome the disadvantages of immune detection, numerous nucleic acid-based techniques have emerged for pathogen detection and identification such as DNA hybridization (Sassolas et al., 2007), polymerase chain reaction (PCR) (Sassolas et al., 2007; Araújo et al., 2012) and DNA microarrays (Sassolas et al., 2007; Araújo et al., 2012; Sharma and Mutharasan, 2013), which

* Corresponding authors.

E-mail addresses: zhouxm@scnu.edu.cn (X. Zhou), xingda@scnu.edu.cn (D. Xing).

offer the advantages of convenience, specificity and sensitivity in the laboratory. Our group had also engaged in using the electrochemiluminescence to detect foodborne pathogens at a gene level (Wei et al., 2010; Long et al., 2011, 2013). Unfortunately, we found that those methods usually require costly instrumentation and skilled personnel, which limit their utility for point-of-care diagnostics under extremely resource-limited environments. Recent studies have employed many isothermal nucleic acid amplifications that can be used to substitute for PCR, such as rolling circle amplification (RCA) (Niemz et al., 2011; Long et al., 2013; Parolo and Merkoci, 2013), strand displacement amplification (SDA) (Foudeh et al., 2012; Yetisen et al., 2013; Hartman et al., 2013), and loop-mediated amplification (LAMP) (Hsieh et al., 2012). These isothermal amplifications provide high specificity and sensitivity, and the elimination of thermal cycling makes these methods more suitable for nucleic acid testing at the point-of-care. While, most of the available isothermal *L. monocytogenes* detection methods still require complex primer design and post-amplification manipulations for detection. Moreover, the isothermal DNA amplification methods are limited in their ability to differentiate between dead and viable pathogens. To address this challenge, more recent molecular detection methods tend to target RNA rather than DNA (Blais et al., 1997; Carter and Cary, 2007; Rohrman et al., 2012). Messenger RNA has a short half-life within nonviable cells, and it is rapidly degraded by enzymes (RNases) that are very stable, even in environments outside the cell itself (Mandin et al., 2007; Reinholt et al., 2013; Fang et al., 2014; Foudeh et al., 2014). The detection of RNA markers would indicate the presence of live cells (Klein and Juneja, 1997; Baeumner et al., 2003).

In this paper, we proposed a new strategy by sensing hlyA mRNA to detect viable pathogenic bacteria. In essence, this *L. monocytogenes* marker was exponentially amplified by one tube isothermal RNA amplification. In our method, this amplification process meets the isothermal requirements and the resulting single-stranded products facilitate the sandwich hybridization-based detection on a paper-based platform. The amplified products could then be simply used for endpoint detection by sandwich hybridization assays using a cheap and instrument free bioactive paper-based platform without the need of complexity of post-amplification manipulations (Martinez et al., 2007, 2009; Liu et al., 2006; Jokerst et al., 2012; Pollock et al., 2012; Song et al., 2014), and gold nanoparticles would then migrate by capillary action and accumulate at the designated Test line and Control line. Finally, the test results can be directly visualized by the naked eye for qualitative observation or by semi-quantitative spectral detection within minutes. Because they are mainly read by the naked eye, this method has great potential for use in the detection of pathogenic bacteria in food, even in the least developed parts of the world, if coupled with the widely used Android-based smart phone and the well-known two-dimensional bar code (Martinez et al., 2008; Smith et al., 2011; Mudanyali et al., 2012; You et al., 2013; Wei et al., 2013; Coskun et al., 2013; Khatua and Orrit, 2013; Feng et al., 2014).

2. Experimental section

2.1. Materials and reagents

An HM3020 X-Z two-dimensional dispenser and GD300 Goldbio cutting module were purchased from Shanghai Goldbio Tech. Co., Ltd. (Shanghai, China). Cellulose fiber sample pads, conjugate pads, plastic adhesive backing pads, absorption pads and nitrocellulose membranes were purchased from Millipore (Billerica, MA). Streptavidin from *Streptomyces avidinii* and Tris (2-carboxyethyl)-phosphine (TCEP) were obtained from Sigma-Aldrich

(St. Louis, MO, USA). Sucrose, sodium phosphate, bovine serum albumin (BSA), formamide, Tween 20, Triton X-100, Tris-HCl, sodium dodecyl sulfate (SDS), dimethyl sulfoxide (DMSO), sodium chloride-sodium citrate (SSC) Buffer 20 × concentrate (pH 7.0), and phosphate buffered saline (PBS, pH 7.4, 0.01 M); RNase H, T7 RNA polymerase, AMV-RT, and their corresponding buffers; ribonuclease inhibitor and deoxynucleotide solution mixture dNTPs (2.5 mM each) were all purchased from Sangon Biotech (Shanghai) Co. Ltd. Sodium chloride (NaCl) and sodium citrate dihydrate were purchased from the Guangzhou Chemical Reagent Factory (Guangzhou, China). Chloroauric acid tetrahydrate ($\text{HAuCl}_4 \cdot 4\text{H}_2\text{O}$) was purchased from Sinopharm Chemical Reagent Co. (Shanghai, China), and RNAiso Plus reagent was received from TaKaRa Biotechnology, Dalian Co., Ltd. (Dalian, China). DNA oligonucleotide probes were obtained from Shanghai Sangon (Shanghai, China). The oligonucleotide sequences are shown in Table S1.

Because all of the reagents were of analytical grade, they were used without further purification. High-purity deionized water (resistance > 18 M Ω cm) was used throughout.

2.2. Preparing the bioactive paper-based platform

The bioactive paper-based platform consists of the following four components: A sample pad, conjugate pad, nitrocellulose membrane, and absorbent pad. All components were mounted on a common plastic adhesive backing pad. The sample pad was made from glass fiber and saturated with a buffer (pH 8.0) containing 0.25% Triton X-100, 0.05 M Tris-HCl, and 0.15 M NaCl. The pad was then dried at 37 °C for 2 h and stored in desiccators at room temperature before use. The AuNPs and AuNP-thiolated DNA probe conjugates which used to embed onto the conjugate pad were prepared with the protocol shown in Supplementary materials (Fig. S1). The Test line and Control line of the bioactive paper-based platforms were prepared by dispensing streptavidin-biotinylated DNA probe solutions onto the nitrocellulose membrane. The streptavidin-biotinylated DNA probes were prepared according to reported methods with slight modifications (Bhatt et al., 2011; Li et al., 2013). In brief, 60 μL of 1 mM biotinylated DNA probes (the sequences of Capture probe T and Capture probe C are shown in Table S1) and 140 μL of PBS were added to 300 μL of 1 mg/mL streptavidin solution, and the mixture was incubated for 1 h at RT. The solutions were then dispensed onto the Test and Control lines of the nitrocellulose membrane with the HM3020 X-Z two-dimensional dispenser. The distance between the Test line and Control line was 5 mm. The membrane was then dried at 37 °C for 1 h and stored at 4 °C in a dry state. Finally, the sample pad, conjugate pad, nitrocellulose membrane, and absorption pad were assembled on a plastic adhesive backing pad. Each part overlapped by 2 mm to ensure the solution was migrating through the bioactive paper during the assay. The bioactive paper platforms with a 4 mm width were cut by using the GD300 Goldbio cutting module.

2.3. Extracting total RNA from bacteria and isothermal RNA amplification

Total RNA was isolated from broth cultures of *L. monocytogenes* bacterial cells with the RNAiso Plus reagent according to the manufacturer's instructions, with some modifications. The detail procedure and the agarose gel results were showed in Supplementary materials (Fig. S2). The isothermal RNA amplification reactions were performed by using the following procedure. A 1 μL sample of RNA was added to 19 μL of isothermal RNA amplification pre-mixture (final concentrations in 20 μL of reaction mixture: 40 mM Tris-HCl, pH 8.5, 12 mM MgCl_2 , 70 mM KCl, certain amount of DMSO, 1 mM of each dNTP, 2 mM of each NTP,

5 × AMV-RT buffer, 5 × T7 RNA polymerase buffer, 10 μM of each primer (primer1 (P1), primer2 (P2); Table S1). The reactions were incubated for 5 min at 65 °C to destabilize the secondary structure of the RNA and subsequently cooled down to 41 °C to allow primer annealing. The amplification reaction was started by adding 5 μL of enzyme mixture (5 × T7 RNA polymerase buffer, 5 × AMV-RT buffer, 10 μg/μL BSA, 5 U/μL RNase H, 20 U/μL T7 RNA polymerase, 10 U/μL AMV-RT, and 40 U/μL ribonuclease inhibitor). Reactions were incubated for 90 min at 41 °C. The isothermal RNA amplification products were stored at −20 °C.

2.4. Detecting artificially contaminated food samples and viability

To obtain quantitative estimates of the detection limits of the paper-based platform for artificially contaminated food samples, raw milk, egg powder, banana, meat and soft cheese samples were chosen as specimens, and they were purchased from local commercial sources. For each specimen, ~25 g of fresh food samples with decreasing amounts of an overnight *L. monocytogenes* culture (100 μL of 10-fold dilutions in peptone water to range from 2 × 10⁴ to 20 CFU/mL) were added to a sterile microcentrifuge tubes, thoroughly mixed and placed on ice for 5 min to sediment the particulate matter. Additionally, 100 μL of 1 × PBS buffer instead of the bacterial strain was added to a food sample, and the mixture was used to perform a negative control experiment. An aliquot of the food sample supernatant (50 μL) was then dispensed into a sterile Eppendorf tube along with 550 μL of lysis buffer (250 μL of TE buffer, 75 μL of 10% sodium dodecyl sulfate (SDS) and 225 μL of benzyl chloride), followed by thorough mixing and incubation at room temperature for 30 min. The total RNA was extracted directly from the lysis buffer-treated food samples with no prior sample enrichment in a final extraction volume of 50 μL and subjected to isothermal RNA amplification.

To monitor the feasibility of differentiating viable bacterial from nonviable ones throughout our method, viable bacteria were treated with a given UV dosage according to the reported method (Klein and Juneja, 1997; Baemner et al., 2003). An overnight pure culture of *L. monocytogenes* was adjusted to a given concentration by gradient dilution (100 μL of 10-fold dilutions in peptone water to range from 2 × 10⁴ to 20 CFU/mL) as positive controls. Additionally, 100 μL of 1 × PBS buffer instead of the bacterial strain was used to perform a negative control experiment. The six samples were plated onto LB agar and cultivated overnight in an incubator at 37 °C. One mL of each sample was removed at the same time for RNA extraction. Finally, all the extracted total RNAs were subjected to isothermal RNA amplification by the above-mentioned process.

2.5. Visual detection of isothermal RNA amplification products with a bioactive paper-based platform

In total, 100 μL of running buffer (4 × SSC+5% formamide+1% SDS+Triton X-100) was mixed with 10 μL of the isothermal RNA amplification product solution in a 1.5 mL centrifuge tube; the mixture was then dispensed onto the sample pad of the bioactive paper-based platform for a rapid test. After waiting for 10 min, 60 μL of running buffer was added to wash the bioactive paper-based platform. The bands were visualized within 5 min. After the test, the results were photographed by a camera installed on an Android-based smart phone. The optical intensities of the red bands on the bioactive paper-based platform were quantified with Image J software, which can determine parameters such as the peak height and area integral. The result was then transformed into a two-dimensional bar code through a conversion website, such as <http://cli.im/img>, to share with distant investigators for further analysis through the telephone, and the results were scanned and re-transformed by two-dimensional bar code

recognition software that was pre-installed on Android-based smart phones.

3. Results and discussion

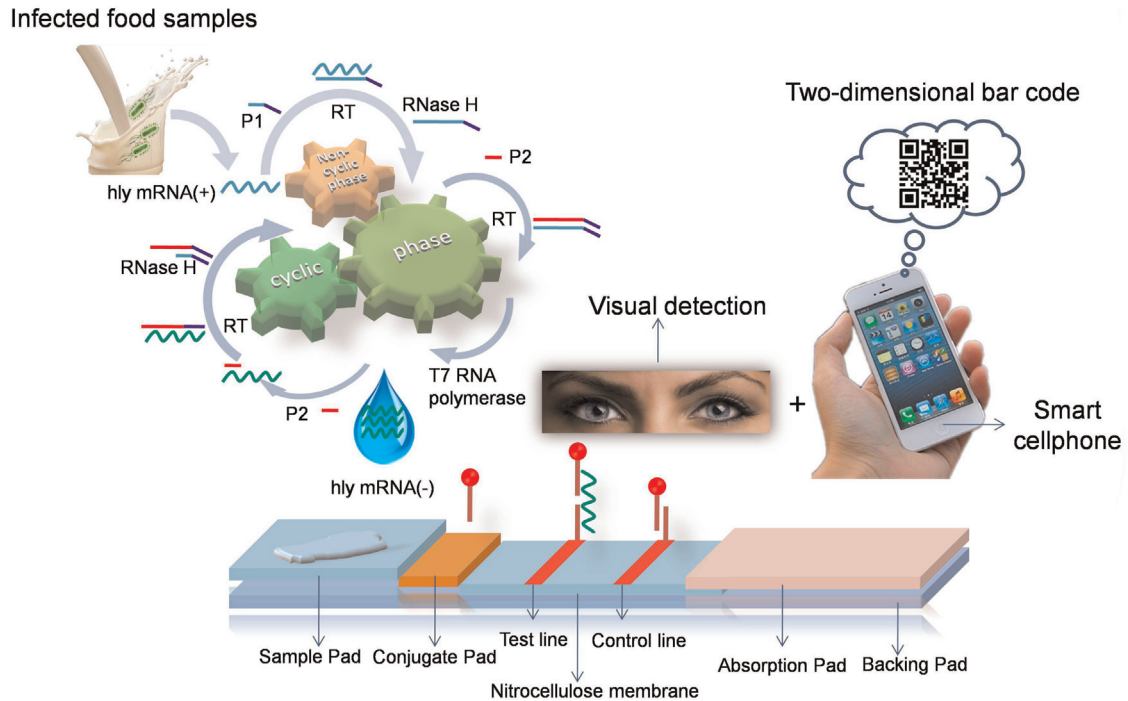
3.1. The principle underlying an isothermal RNA amplification-based and bioactive paper-based platform for detecting pathogenic bacteria

We initially sought to develop an on-site, in-field technique for detecting viable pathogenic bacteria. Unfortunately, the utility of paper-based detection in the context of a classical PCR-based assay is severely limited by a reliance on thermocycling hardware. This approach largely negates the potential benefit of the otherwise highly simplified paper-based platform. Additionally, the double-stranded PCR products required an additional annealing and hybridization procedure for sandwich hybridization-based detection on a paper-based platform. To avoid the complexity of post-amplification manipulations and increase the potential applications available with easy accessibility, an isothermal RNA amplification-based paper detection platform was developed. Comparison between Current isothermal RNA amplification and other amplification methods for *Listeria* detection was showed in the Supplementary material (Table S2).

This amplification process meets the isothermal requirements and is able to produce single-stranded products (shown in Fig. S3). First, in “non-cyclic phase”, primer 1 (P1) anneals to the original single-stranded RNA template, and its 3′ terminus is extended by AMV reverse transcriptase, forming a cDNA copy of the template and resulting in a DNA hybrid. RNase H then hydrolyses the RNA from the DNA hybrid, leaving a single strand of DNA to which primer 2 anneals. Reverse transcriptase synthesizes the second DNA strand, rendering the promoter region double-stranded. Finally, T7 RNA polymerase transcribes RNA copies from the promoter, generating as many as 100 copies from each template molecule. Each new RNA molecule then acts as a template for reverse transcriptase in the “cyclic phase” isothermal RNA amplification process. In the following process, this fascinating process ensures a 10⁹-fold exponential amplification of each target within 90 min (Blais et al., 1997; Carter and Cary, 2007; Rohrman et al., 2012). Finally, the product of the isothermal RNA amplification reaction is primarily single-stranded RNA, facilitating a rapid test using the bioactive paper-based platform.

The principle underlying this bioactive paper-based platform measurement is an on-paper sandwich DNA hybridization reaction and the accumulation of gold nanoparticles at designated Test lines and Control lines when migrating along the bioactive paper by capillary action (Park et al., 2002; Cao et al., 2011; Lei and Ju, 2012); the protocol is illustrated in Scheme 1.

The resultant single-stranded products mixed with running buffer are applied to the bioactive paper-based platform. As the mixture liquid migrates along the bioactive paper-based platform to the conjugate pad, it then rehydrates the AuNP–thiolated DNA probe conjugates. The target RNA hybridizes with the thiolated DNA probe of the AuNP–thiolated DNA probe conjugates to form the complex and continues to migrate along the strip. The hybrids are captured on the Test line by the second hybridization between the target RNA and immobilized capture probe T. The accumulation of AuNPs on the Test line of the nitrocellulose membrane is visualized as a characteristic red band. The excess conjugates of the AuNP–thiolated DNA probe continue to migrate and pass the Control line, in which capture probe C is immobilized. The excess AuNP–thiolated DNA probe conjugates are captured by the hybridization events between the thiolated DNA probe and capture probe C, thus forming a second red band. In the absence of target RNA, no red band is observed in the Test line.



Scheme 1. Schematic illustration of isothermal RNA amplification and the configuration of the bioactive paper-based platform.

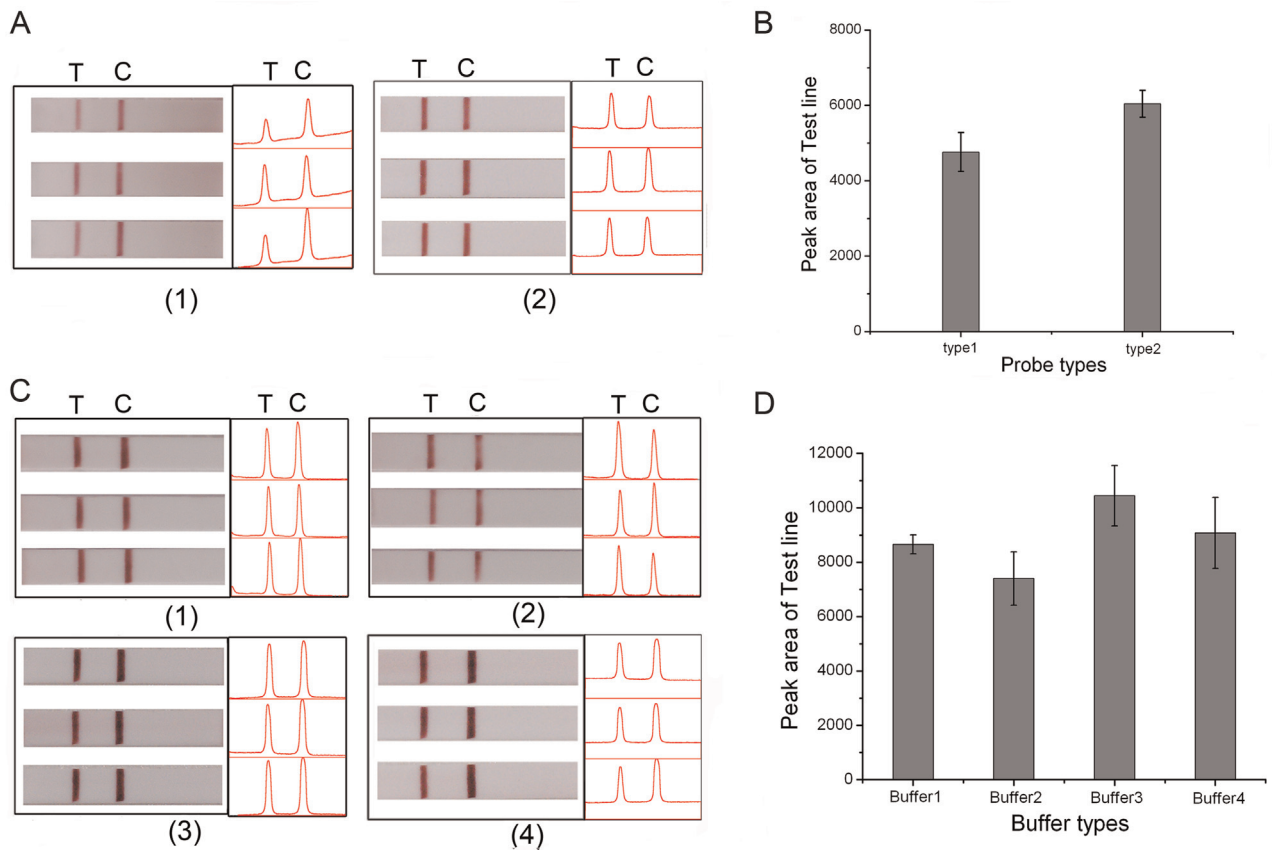


Fig. 1. Key parameters that affected the performance of the bioactive paper-based platform. (A) The effects of different probe types used during the preparation of AuNP–DNA conjugates on the response of 50 pg/μL target RNA from *Listeria monocytogenes* in the bioactive paper-based platform: (1) probe type 1, which is missing the Poly(A)₁₂ linker at the 5' terminus of the probe, was used during the preparation of AuNP–DNA conjugates and resulted in reddish bands on the Test lines and Control lines, (2) probe type 2, which has a Poly(A)₁₂ linker at the 5' terminus of the probe, yielded deeper red bands on the Test lines and Control lines. (B) The histogram of optical intensities on the Test line with the two probe types. (C) The effects of different types of running buffer on the response of 50 pg/μL target *Listeria monocytogenes*: (1) buffer 1: 4 × SSC + 5% formamide, (2) buffer 2: 4 × SSC, (3) buffer 3: 4 × SSC + 5% formamide + 1% SDS, (4) buffer 4: 4 × SSC + 5% formamide + 1% SDS + Triton X-100. (D) A histogram of the optical intensities on the Test line with the four types of buffer. (For interpretation of the references to color in this figure legend, the reader is referred to the web version of this article.)

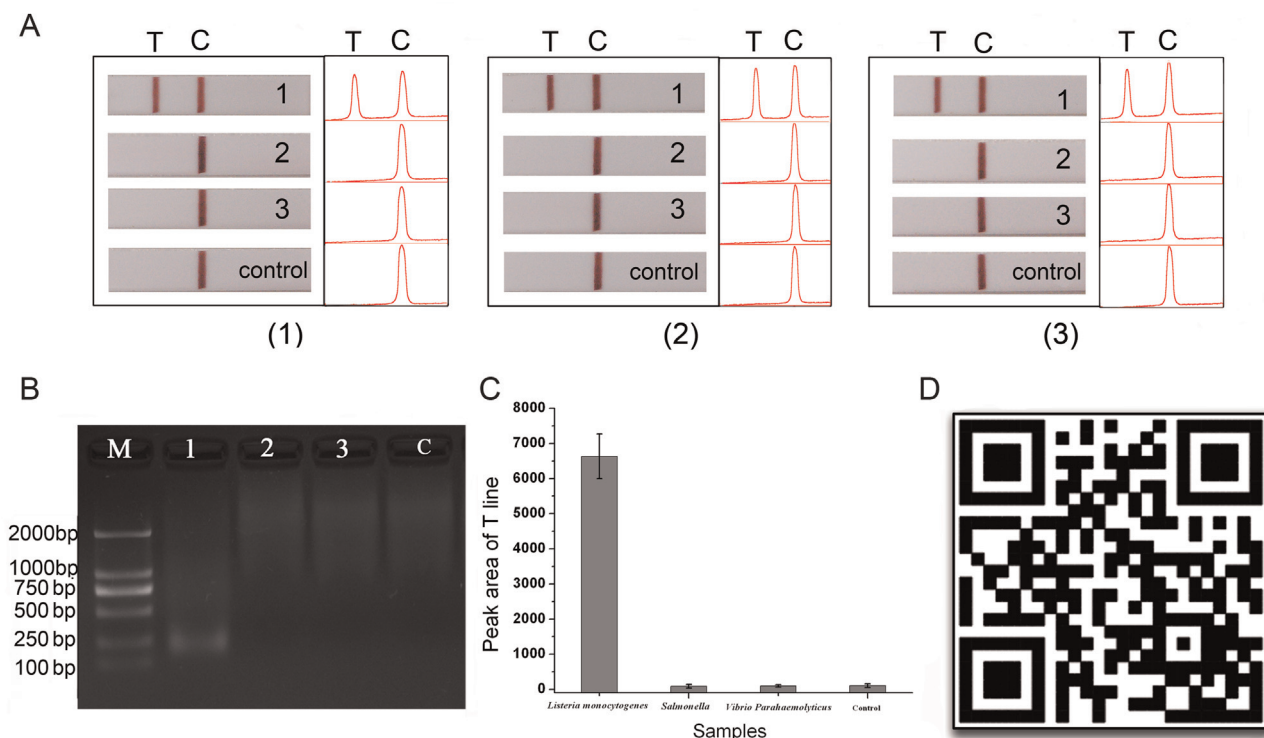


Fig. 2. Specificity evaluation of the bioactive paper-based platform. (A) (1)–(3) represent the triplicate test results for the samples and the corresponding optical response of the Test and Control lines on each paper platform, strip 1: paper-based test results for *Listeria monocytogenes*; strip 2 and 3: paper-based test results for *Vibrio parahaemolyticus* and *Salmonella*; strip C: paper-based test results for the negative control. (B) Gel electrophoresis (1%) to identify the current specificity evaluation; line 1 shows the amplification products of the hlyA mRNA from *Listeria monocytogenes* (133-mer), and lines 2 and 3 show that the *Listeria monocytogenes* primers did not amplify *Vibrio parahaemolyticus* and *Salmonella*, respectively; the result of the control is negative. (C) Optical intensities of the Test lines for the results; the obvious intensities in the histogram correspond to *Listeria monocytogenes*. (D) Transformed two-dimensional bar code from the raw picture (attached in the [Supplementary materials \(Fig. S5\)](#)) of the current specificity evaluation.

After the test, the bioactive paper-based platform was imaged by the camera installed in the Android-based smart phone. The optical intensities of the Test and Control lines were recorded simultaneously using Image J software, which can determine parameters such as the peak height and area integral. The result could then be transformed into two-dimensional bar codes to share with distant investigators for further analysis using a telephone, which can scan and retransform the result using scan software pre-installed on Android-based smart phones.

3.2. Key parameters of the isothermal RNA amplification-based, bioactive paper-based platform in current assay

In this experiment, we found that the DMSO concentration was a very important factor in the amplification of isothermal RNA. Adding DMSO to the reaction mixture increased the activity of AMV reverse transcriptase and RNaseH. It was also helpful for opening the RNA secondary structure, as it improved the specificity and promoted the reaction speed and stability of the isothermal RNA amplification. A 1% agarose gel electrophoresis analysis of the isothermal RNA amplification product was performed in this experiment. As shown in [Supplementary materials \(Fig. S4\)](#), the corresponding amplified results were obtained when the DMSO concentrations were 9%, 11%, 13%, 15% and 17%. There is a distinct band in lane 4 when compared with the other lanes, indicating that the amplification efficiency was higher when the DMSO concentration was 15%. Therefore, a DMSO concentration of 15% was selected as the optimum condition for later isothermal RNA amplification.

As shown in [Fig. 1\(A\)](#), the intensity of the Test line increased markedly in the presence of the Poly (A)₁₂ of the probe used

during the preparation of AuNP–DNA conjugates in response to 50 pg/μL target hlyA mRNA on the bioactive paper-based platform. Furthermore, we found that the presence of a Poly (A)₁₂ linker at the 5' terminus of the probe markedly improved the test's efficiency when used during the preparation of AuNP–DNA conjugates. We therefore infer that the presence of Poly (A)₁₂ in the probe can reduce the steric hindrance effect of the sandwich hybridization reaction between AuNP–DNA conjugates and streptavidin-biotinylated DNA probes on the Test and Control lines of the bioactive paper-based platform.

The running buffer used in such a test can critically affect the performance of the sensors, and using the optimal buffers would minimize nonspecific adsorption and increase the sensitivity and reproducibility of the bioactive paper-based platform. We therefore compared the performance of the bioactive paper-based platform tests using different running buffers, including 4 × SSC; 4 × SSC+5% formamide; 4 × SSC+5% formamide+1% SDS; and 4 × SSC+5% formamide+1% SDS+Triton X-100. We found that the 4 × SSC+5% formamide+1% SDS buffer provided the best performance (results shown in [Fig. 1\(B\)](#)).

3.3. The specificity and sensitivity of the current assay

The specificity of our strategy was examined under optimized experimental conditions. Total RNA was diluted to 50 pg/μL following extraction from pure broth cultures of *L. monocytogenes*, *Vibrio parahaemolyticus* and *Salmonella*. As shown in the images of triplicate tests in [Fig. 2\(A\)](#), a positive result yielded reddish-purple bands at the Test and Control lines, whereas a negative result yielded reddish-purple bands at the Control lines only. [Fig. 2\(B\)](#) shows that no amplification reactions were observed in the

assays of any of the non-*Listeria* bacteria (line 2, 3) or the control (line 4), but a distinct band was observed in the assays with the *Listeria* bacteria (line 1). The cartogram in Fig. 2(C) is consistent with the gel electrophoresis and paper-based platform results. Fig. 2(D) demonstrates the feasibility of using a two-dimensional bar code as receiving/transmitting media for rapid specific testing. These results confirm that the targeted hlyA mRNA sequences are specific for *L. monocytogenes* and that the isothermal RNA amplification-hybridization assay should be sufficiently discriminatory to enable the detection of this pathogen in test samples such as foods.

Different concentrations of target RNA from *L. monocytogenes* were tested to evaluate the sensitivity of the isothermal RNA amplification reaction-based, bioactive paper-based platform detection method. Fig. 3(A) presents typical photo images from the bioactive paper-based platform in the presence of target RNA concentrations of 0.5 pg/ μ L, 5 pg/ μ L, 50 pg/ μ L and 500 pg/ μ L. There is an obvious and continuous increase in the intensity of the test zone as the amount of target RNA increases. Fig. 3(B) shows that analysis of isothermal RNA amplification reactions from different concentrations of target RNA by electrophoresis; lines 1–4 are 500 pg/ μ L, 50 pg/ μ L, 5 pg/ μ L, and 0.5 pg/ μ L, respectively and lines 5 is the negative control. The cartogram in Fig. 3(C) is consistent with the gel electrophoresis and paper-based platform results. The peaks in the figure represent for the intensity of the Test line of each strip. There is a linear relationship between peak height or area with the concentration of target ($R^2=0.99886$). Fig. 3(D) confirms the feasibility of using a two-dimensional bar code as receiving/transmitting media for rapid sensitive testing. These

results well demonstrate the extraordinary capability of our isothermal RNA amplification-hybridization assay platform in detecting *L. monocytogenes*. In addition, the sensitivity was higher than previously reported in nucleic acid-based detection platforms for food-borne pathogenic bacteria (Baeumner et al., 2003; Ngom et al., 2010).

3.4. Detecting artificially contaminated samples using the bioactive paper-based platform

To evaluate the platform's ability to detect pathogenic bacteria in food, total RNA was extracted directly from artificially contaminated raw milk, egg powder, bananas, meat and soft cheese samples with no prior sample enrichment and then subjected to isothermal RNA amplification.

Fresh food samples with decreasing amounts of an overnight *L. monocytogenes* culture (100 μ L of 10-fold dilutions in peptone water to range from 2×10^4 to 2×10^2 CFU/mL) all gave positive results. Fig. 4(A) indicates that the raw milk (line 1), banana (line 2) and meat (line 3) samples that were inoculated with *L. monocytogenes* at a level of 20 CFU/mL produced an expected isothermal RNA amplification signal, whereas non-specific amplification results were apparently obtained from the egg powder (line 4) and soft cheese (line 5) samples that were also inoculated with *L. monocytogenes* at a level of 20 CFU/mL. Fig. 4(B) shows the corresponding test results from the paper-based platform. The Test line intensity for the raw milk, banana and meat samples were distinct, and reddish-purple bands were observed on the Test line for the egg powder and soft cheese samples. It is possible that the

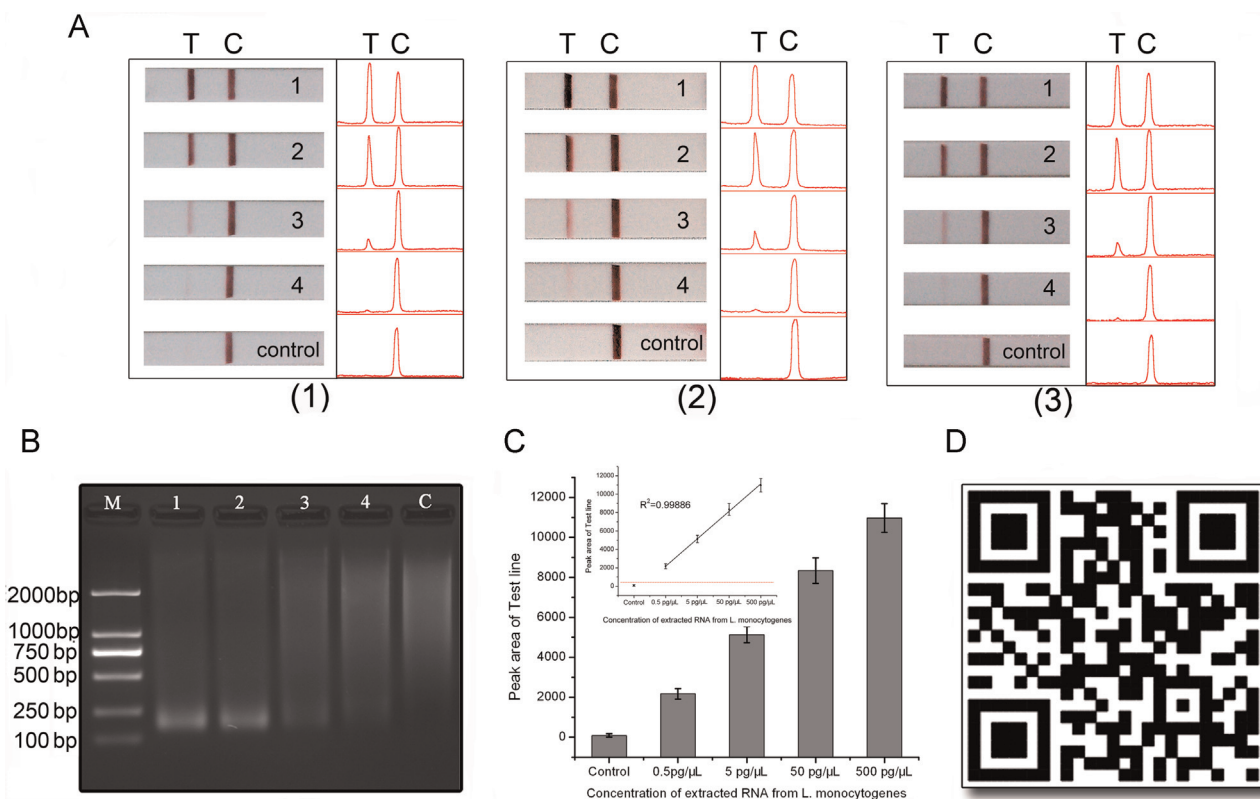


Fig. 3. Sensitivity assay of the bioactive paper-based platform. (A) Typical photo images of the test results on the bioactive paper-based platform and the corresponding optical response of the Test and Control lines on each paper platform; (1)–(3) represent the triplicate test results of the different target RNA concentrations: strip 1: 500 pg/ μ L, strip 2: 50 pg/ μ L, strip 3: 5 pg/ μ L, strip 4: 0.5 pg/ μ L, and strip C: negative control. (B) Analysis of isothermal RNA amplification reactions from different concentrations of target RNA by electrophoresis; lines 1–4 are 500 pg/ μ L, 50 pg/ μ L, 5 pg/ μ L, and 0.5 pg/ μ L, respectively. (C) The sensitivity assessment of the bioactive paper-based platform. (D) transformed two-dimensional bar code from the raw picture (attached in the Supplementary materials (Fig. S6)) of the current sensitivity assay. (For interpretation of the references to color in this figure, the reader is referred to the web version of this article.)

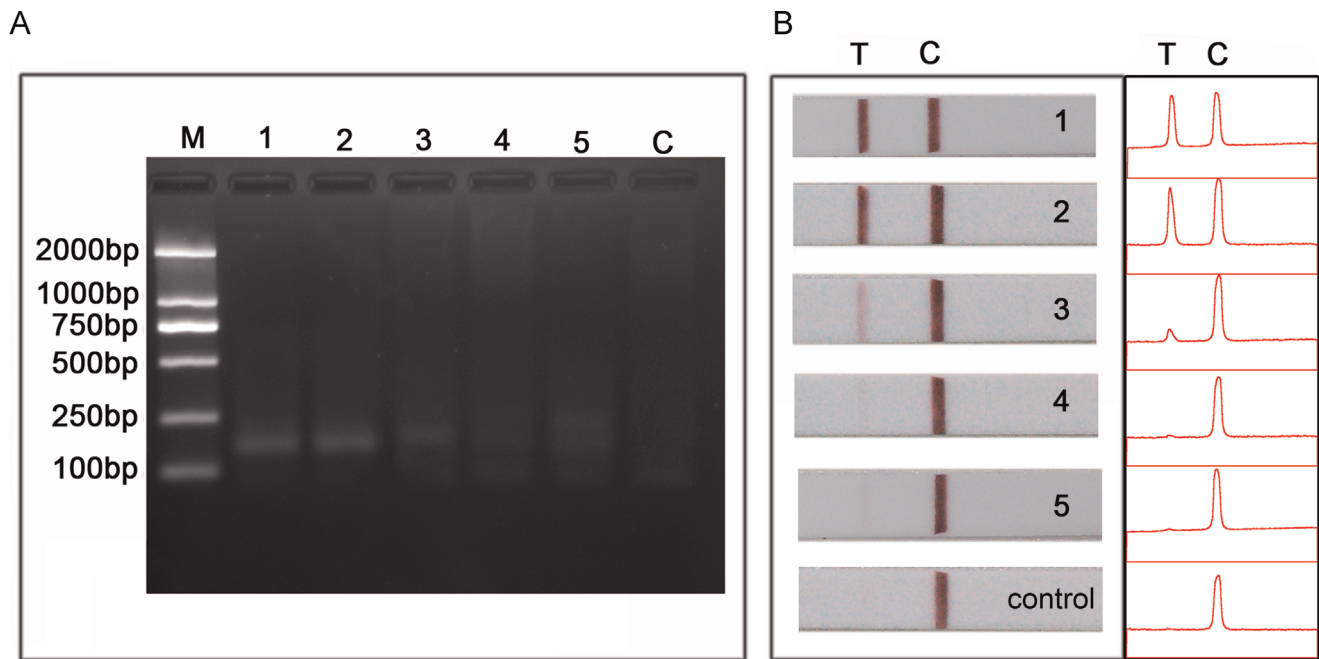


Fig. 4. Detection results for artificially contaminated samples with the bioactive paper-based platform. (A) Gel electrophoresis (1%) to identify artificially contaminated raw milk, egg powder, banana, meat and soft cheese samples with *Listeria monocytogenes* from line 1 to line 5, and line C is the negative control of the current assay. (B) Typical photo images of the detection results of different food samples and the corresponding optical response of the Test and Control lines on each paper platform. (For interpretation of the references to color in this figure, the reader is referred to the web version of this article.)

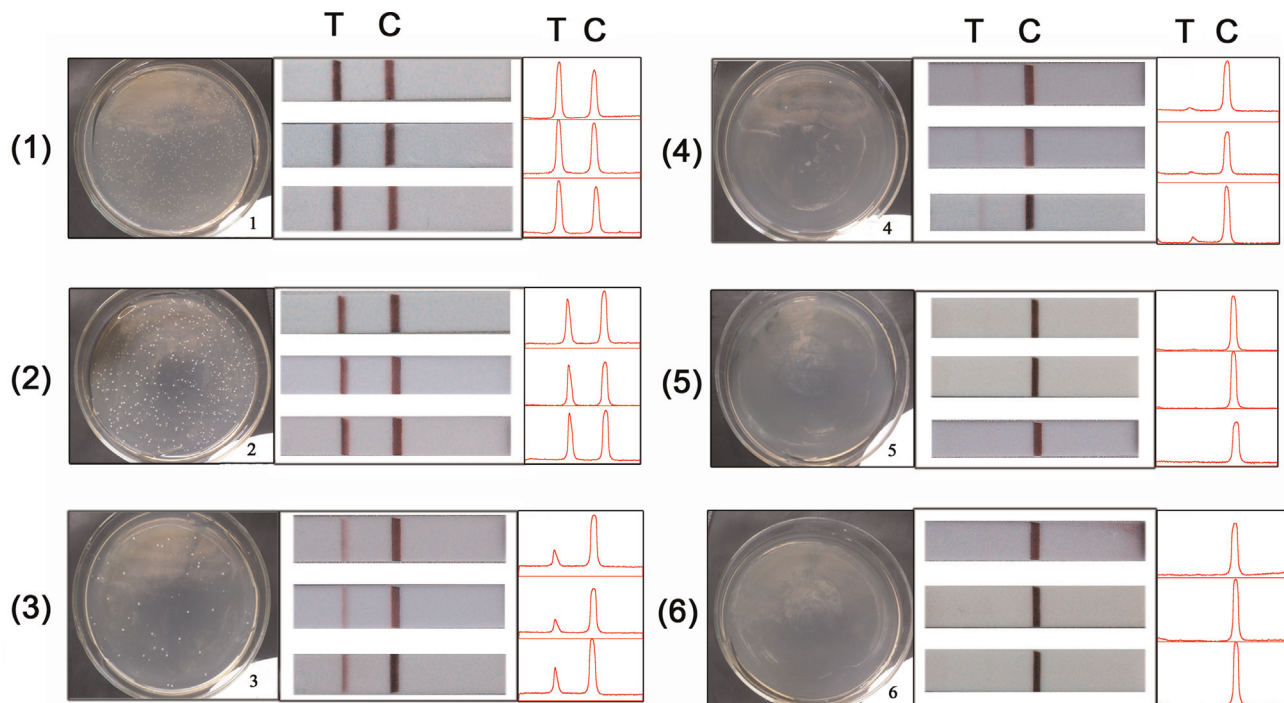


Fig. 5. mRNA detection as a viability indicator in *Listeria monocytogenes*. (1)–(4) The test results for different concentrations of *Listeria monocytogenes* with gradient dilutions plated onto agar, and the naked-eye observation result on the paper-based platform; although there is a continuous decrease in the intensity of the Test line with the positive controls from 2×10^4 CFU/mL to 20 CFU/mL, the numbers of cultivated bacteria plated onto LB agar decrease as well. (5) and (6) Test results for nonviable bacterial pathogens and the negative control detection both on the platform and the agar; no red band is visible at the Test line with the UV-treated sample or the control sample, and the test results were consistent with the cultivation results for the treated bacteria plated onto LB agar and the negative control sample, in which no viable cells were detected. The corresponding optical response of the Test and Control lines on each paper platform clearly demonstrates this trend. (For interpretation of the references to color in this figure, the reader is referred to the web version of this article.)

residual food components from the two dry samples inhibited the isothermal enzymatic reactions or mixed into the DNA when the RNA was isolated from the two dry samples. Further purifications of the isolated RNA could improve the amplification efficiency and prevent false-negative results. Further interference test with real samples were also conducted to demonstrate the selectivity of the proposed isothermal RNA amplification based paper platform for pathogenic bacteria detection. (the results were showed in [Supplementary material \(Fig. S7\)](#)).

3.5. Detecting mRNA as a viability indicator in *L. monocytogenes*

To monitor the feasibility of differentiating viable bacteria from nonviable bacteria using our method, we simulated the detection of viable and nonviable bacteria (killed by UV) in robust environments using the current RNA-based method. Pure cultures of *L. monocytogenes* grown overnight and subjected to gradient dilution were used as positive controls. [Fig. 5](#) shows that no red band appeared at the Test line for the UV-treated and negative control samples. After a certain dosage of UV treated, UV-light damages the DNA of the *L. monocytogenes* by forming thymine dimers, which prevent the *L. monocytogenes* from DNA transcription and replication which leads to cell death ([Ozer and Demirci, 2006](#); [Bank et al., 1990](#)). So the target RNA markers of the *L. monocytogenes* could not be isolated from the broth cultures of *L. monocytogenes* bacterial cells, and the isothermal amplification would not be triggered. When applied the reaction mixtures to the paper-based platform, the sandwich hybridization reaction and accumulation of gold nanoparticles at designated Test lines would not happen. The test results were consistent with the cultivation result of the treated bacteria when plated onto LB agar and the negative control sample in which no viable cells were detected. There is a continuous decrease in the intensity of the Test line for positive controls, and the status of the cultivated bacteria that were plated onto LB agar clearly demonstrated this tendency. It was possible to confirm that the isothermal RNA amplification-based bioactive paper-based platform was reliable for the visual and sensitive detection of viable pathogenic bacteria.

4. Conclusions

In summary, we have demonstrated a simple and sensitive method for the visual detection of viable pathogenic bacteria based on an isothermal RNA amplification reaction-based bioactive paper-based platform employing a two-dimensional bar code as the receiving/transmitting media for a rapid test. The platform performance effects of the reaction parameters, including the DMSO concentration, probe types and buffer types, have been experimentally evaluated. The assay takes advantage of the high isothermal amplification efficiency of the isothermal RNA amplification reaction and the portable bioactive paper-based platform. It has a limit of detection of 0.5 pg/μL genomic RNA from viable *L. monocytogenes* with a high specificity within 15 min. In addition, it can be used specifically to detect 20 CFU/mL *L. monocytogenes* from actual samples such as milk and cheese. The viability experiment confirmed that this strategy was reliable for the visual and sensitive detection of viable pathogenic bacteria. We also introduced the two-dimensional bar code as receiving/transmitting media for the first time; thus, the test results can be transmitted, received and shared with distant investigators for faster additional analysis. This portable, integrated test model holds great promise for point-of-care and in-field analyses of other food-borne pathogenic bacteria, by making slight modification.

Acknowledgments

This research was supported by the National Basic Research Program of China (2010CB732602), the Key Program of NSFC–Guangdong Joint Funds of China (U0931005), the Program of the Pearl River Young Talents of Science and Technology in Guangzhou, China (2013J2200021) and the National Natural Science Foundation of China (81101121).

Appendix A. Supplementary material

Supplementary data associated with this article can be found in the online version at <http://dx.doi.org/10.1016/j.bios.2014.06.020>.

References

- Araújo, A.C., Song, Y., Lundeberg, J., Ståhl, P.L., Brumer, H., 2012. *Anal. Chem.* 84 (7), 3311–3317.
- Bank, John, H.L., Schmehl, J., Dratch, R.J., M.K., 1990. *Appl. Environ. Microbiol.* 56 (12), 3888–3889.
- Baummer, A.J., Cohen, R.N., Miksic, V., Min, J., 2003. *Biosens. Bioelectron.* 18 (4), 405–413.
- Bhatt, N., Huang, P.-J.J., Dave, N., Liu, J., 2011. *Langmuir* 27 (10), 6132–6137.
- Birmingham, C.L., Canadien, V., Kaniuk, N.A., Steinberg, B.E., Higgins, D.E., Brumell, J. H., 2008. *Nature* 451 (7176), 350–354.
- Blais, B.W., Turner, G., Sooknanan, R., Malek, L.T., 1997. *Appl. Environ. Microbiol.* 63 (1), 310–313.
- Cao, C., Gontard, L.C., Thuy Tram, L.L., Wolff, A., Bang, D.D., 2011. *Small* 7 (12), 1701–1708.
- Carter, D.J., Cary, R.B., 2007. *Nucleic Acids Res.* 35 (10), e74.
- Cho, I.-H., Irudayaraj, J., 2013. *Anal. Bioanal. Chem.* 405 (10), 3313–3319.
- Coskun, A.F., Wong, J., Khodadadi, D., Nagi, R., Tey, A., Ozcan, A., 2013. *Lab Chip* 13 (4), 636–640.
- Cossart, P., Toledo-Arana, A., 2008. *Microbes Infect.* 10 (9), 1041–1050.
- Fang, Z., Wu, W., Lu, X., Zeng, L., 2014. *Biosens. Bioelectron.* 56 (0), 192–197.
- Feng, S., Caire, R., Cortazar, B., Turan, M., Wong, A., Ozcan, A., 2014. *ACS Nano* 8 (3), 3069–3079.
- Foudeh, A.M., Daoud, J.T., Faucher, S.P., Veres, T., Tabrizian, M., 2014. *Biosens. Bioelectron.* 52 (0), 129–135.
- Foudeh, A.M., Fatanat Didar, T., Veres, T., Tabrizian, M., 2012. *Lab Chip* 12 (18), 3249–3266.
- Ge, L., Yan, J., Song, X., Yan, M., Ge, S., Yu, J., 2012. *Biomaterials* 33 (4), 1024–1031.
- Hamon, M., Bierne, H., Cossart, P., 2006. *Nat. Rev. Microbiol.* 4 (6), 423–434.
- Hartman, M.R., Ruiz, R.C.H., Hamada, S., Xu, C., Yancey, K.G., Yu, Y., Han, W., Luo, D., 2013. *Nanoscale* 5 (21), 10141–10154.
- Hsieh, K., Patterson, A.S., Ferguson, B.S., Plaxco, K.W., Soh, H.T., 2012. *Angew. Chem. Int. Ed.* 51 (20), 4896–4900.
- Hsu, M.Y., Yang, C.Y., Hsu, W.H., Lin, K.H., Wang, C.Y., Shen, Y.C., Chen, Y.C., Chau, S.F., Tsai, H.Y., Cheng, C.M., 2014. *Biomaterials* 35 (12), 3729–3735.
- Jokerst, J.C., Adkins, J.A., Bisha, B., Mentele, M.M., Goodridge, L.D., Henry, C.S., 2012. *Anal. Chem.* 84 (6), 2900–2907.
- Klein, P.G., Juneja, V.K., 1997. *Appl. Environ. Microbiol.* 63 (11), 4441–4448.
- Khatua, S., Orrit, M., 2013. *ACS Nano* 7 (10), 8340–8343.
- Lei, J., Ju, H., 2012. *Chem. Soc. Rev.* 41 (6), 2122–2134.
- Li, F., Zhang, H., Dever, B., Li, X.-F., Le, X.C., 2013. *Bioconj. Chem.* 24 (11), 1790–1797.
- Liu, J., Mazumdar, D., Lu, Y., 2006. *Angew. Chem. Int. Ed.* 118 (47), 8123–8127.
- Long, Y., Zhou, X., Xing, D., 2011. *Biosens. Bioelectron.* 26 (6), 2897–2904.
- Long, Y., Zhou, X., Xing, D., 2013. *Biosens. Bioelectron.* 46, 102–107.
- Mandini, P., Repoila, F., Vergassola, M., Geissmann, T., Cossart, P., 2007. *Nucleic Acids Res.* 35 (3), 962–974.
- Martinez, A.W., Phillips, S.T., Butte, M.J., Whitesides, G.M., 2007. *Angew. Chem. Int. Ed.* 46 (8), 1318–1320.
- Martinez, A.W., Phillips, S.T., Carrilho, E., Thomas, S.W., Sindi, H., Whitesides, G.M., 2008. *Anal. Chem.* 80 (10), 3699–3707.
- Martinez, A.W., Phillips, S.T., Whitesides, G.M., Carrilho, E., 2009. *Anal. Chem.* 82 (1), 3–10.
- Mudanyali, O., Dimitrov, S., Sikora, U., Padmanabhan, S., Navruz, I., Ozcan, A., 2012. *Lab Chip* 12 (15), 2678–2686.
- Nash, M.A., Waitumbi, J.N., Hoffman, A.S., Yager, P., Stayton, P.S., 2012. *ACS Nano* 6 (8), 6776–6785.
- Ngom, B., Guo, Y., Wang, X., Bi, D., 2010. *Anal. Bioanal. Chem.* 397 (3), 1113–1135.
- Niemz, A., Ferguson, T.M., Boyle, D.S., 2011. *Trends Biotechnol.* 29 (5), 240–250.
- Ozer, N.P., Demirci, A., 2006. *Int. J. Food Sci. Technol.* 41 (4), 354–360.
- Park, S.-J., Taton, T.A., Mirkin, C.A., 2002. *Science* 295 (5559), 1503–1506.
- Parolo, C., Merkoci, A., 2013. *Chem. Soc. Rev.* 42 (2), 450–457.
- Pollock, N.R., Rolland, J.P., Kumar, S., Beattie, P.D., Jain, S., Noubary, F., Wong, V.L., Pohlmann, R.A., Ryan, U.S., Whitesides, G.M., 2012. *Sci. Transl. Med.* 4 (152), 152ra129.

- Reinholt, S.J., Behrent, A., Greene, C., Kalfe, A., Baeumner, A.J., 2013. *Anal. Chem.* 86 (1), 849–856.
- Ribet, D., Hamon, M., Gouin, E., Nahori, M.-A., Impens, F., Neyret-Kahn, H., Gevaert, K., Vandekerckhove, J., Dejean, A., Cossart, P., 2010. *Nature* 464 (7292), 1192–1195.
- Rivoal, K., Fablet, A., Courtyllon, C., Bougeard, S., Chemaly, M., Protais, J., 2013. *Int. J. Food Microbiol.* 166 (1), 109–116.
- Rohrman, B.A., Leautaud, V., Molyneux, E., Richards-Kortum, R.R., 2012. *PLoS One* 7 (9), e45611.
- Rood, J.I., 2010. *Nature* 464 (7292), 1138–1139.
- Sassolas, A., Leca-Bouvier, B.D., Blum, L.J., 2007. *Chem. Rev.* 108 (1), 109–139.
- Shafiee, H., Jahangir, M., Inci, F., Wang, S., Willenbrecht, R.B.M., Giguel, F.F., Tsibris, A.M.N., Kuritzkes, D.R., Demirci, U., 2013. *Small* 9 (15), 2553–2563.
- Sharma, H., Mutharasan, R., 2013. *Anal. Chem.* 85 (6), 3222–3228.
- Smith, Z.J., Chu, K., Espenson, A.R., Rahimzadeh, M., Gryshuk, A., Molinaro, M., Dwyre, D.M., Lane, S., Matthews, D., Wachsmann-Hogiu, S., 2011. *PLoS One* 6 (3), e17150.
- Song, Y., Gyarmati, P., Araújo, A.C., Lundeberg, J., Brumer, H., Ståhl, P.L., 2014. *Anal. Chem.* 86 (3), 1575–1582.
- Wei, J., Zhou, X., Xing, D., Wu, B., 2010. *Food Chem.* 123 (3), 852–858.
- Wei, Q., Qi, H., Luo, W., Tseng, D., Ki, S.J., Wan, Z., Göröcs, Z., Bentolila, L.A., Wu, T.-T., Sun, R., Ozcan, A., 2013. *ACS Nano* 7 (10), 9147–9155.
- Yan, J., Ge, L., Song, X., Yan, M., Ge, S., Yu, J., 2012. *Chem. Eur. J.* 18 (16), 4938–4945.
- Yetisen, A.K., Akram, M.S., Lowe, C.R., 2013. *Lab Chip* 13 (12), 2210–2251.
- You, D.J., Park, T.S., Yoon, J.-Y., 2013. *Biosens. Bioelectron.* 40 (1), 180–185.
- Zunabovic, M., Domig, K.J., Kneifel, W., 2011. *LWT—Food Sci. Technol.* 44 (2), 351–362.